Intracellular label-free gold nanorods imaging with photoacoustic microscopy

Sihua Yang, Fei Ye, and Da Xing*

MOE Key Laboratory of Laser Life Science & Institute of Laser Life Science, College of Biophotonics, South China Normal University, Guangzhou 510631,China

*xingda@scnu.edu.cn

Abstract: Noninvasive photoacoustic microscopy was developed to image intracellular gold nanorods with high optical-absorption contrast. The endocytosed gold nanorods in MCF7 cells can be detected and imaged with the home-made photoacoustic microscope. Cell nucleus and gold nanorods in cytoplasm were clearly identified after hematoxylin and eosin (H&E) staining with dual-wavelength excitation. The intracellular gold nanorods were successfully monitored, and that the time-dependent uptake and distribution of the gold nanorods in the cells were clearly shown. The result demonstrated an application of photoacoustic microscopy for complements to imaging of nonfluorescent nanoparticles, which will arm the *in vivo* microscopic imaging method to the nano-bio research.

OCIS codes: (110.5120) Photoacoustic imaging; (110.7170) Ultrasound; (170.3880) Medical and biological imaging.

References and links

1. L. Tong, Q. Wei, A. Wei, and J. X. Cheng, "Gold nanorods as contrast agents for biological imaging: optical properties, surface conjugation and photothermal effects," Photochem. Photobiol. **85**(1), 21–32 (2009).
2. O. Schwartz and D. Oron, "Background-free third harmonic imaging of gold nanorods," Nano Lett. **9**(12), 4093–4097 (2009).
3. T. B. Huff, M. N. Hansen, Y. Zhao, J. X. Cheng, and A. Wei, "Controlling the cellular uptake of gold nanorods," Langmuir **23**(4), 1596–1599 (2007).
4. X. Huang, I. H. El-Sayed, W. Qian, and M. A. El-Sayed, "Cancer cell imaging and photothermal therapy in the near-infrared region by using gold nanorods," J. Am. Chem. Soc. **128**(6), 2115–2120 (2006).
5. H. Xu, W. Dai, Y. Han, W. Hao, F. Xiong, Y. Zhang, and J. M. Cao, "Differential internalization of superparamagnetic iron oxide nanoparticles in different types of cells," J. Nanosci. Nanotechnol. **10**(11), 7406–7410 (2010).
6. D. L. Farkas, D. V. Nicolau, and R. C. Leif, "Gold nanorods for cell imaging with confocal reflectance microscopy and two-photon fluorescence microscopy," Proc. SPIE **7568**, 75680A (2010).
7. N. J. Durr, T. Larson, D. K. Smith, B. A. Korgel, K. Sokolov, and A. Ben-Yakar, "Two-photon luminescence imaging of cancer cells using molecularly targeted gold nanorods," Nano Lett. **7**(4), 941–945 (2007).
8. H. Wang, T. B. Huff, D. A. Zweifel, W. He, P. S. Low, A. Wei, and J. X. Cheng, "In vitro and in vivo two-photon luminescence imaging of single gold nanorods," Proc. Natl. Acad. Sci. U.S.A. **102**(44), 15752–15756 (2005).
9. C. W. Freudiger, W. Min, B. G. Saar, S. Lu, G. R. Holtom, C. He, J. C. Tsai, J. X. Kang, and X. S. Xie, "Label-free biomedical imaging with high sensitivity by stimulated Raman scattering microscopy," Science **322**(5909), 1857–1861 (2008).
10. A. Gaiduk, M. Yorulmaz, P. V. Ruijgrok, and M. Orrit, "Room-temperature detection of a single molecule's absorption by photothermal contrast," Science **330**(6002), 353–356 (2010).
11. V. P. Zharov, "Ultrasharp nonlinear photothermal and photoacoustic resonances and holes beyond the spectral limit," Nat. Photonics **5**(2), 110–116 (2011).
12. D. A. Nedosekin, E. I. Galanzha, S. Ayyadevara, R. J. Shmookler Reis, and V. P. Zharov, "Photothermal confocal spectromicroscopy of multiple cellular chromophores and fluorophores," Biophys. J. **102**(3), 672–681 (2012).
13. L. V. Wang, "Multiscale photoacoustic microscopy and computed tomography," Nat. Photonics **3**(9), 503–509 (2009).
14. D. Razansky, M. Distel, C. Vinegoni, R. Ma, N. Perrimon, R. W. Köster, and V. Ntziachristos, "Multispectral opto-acoustic tomography of deep-seated fluorescent proteins in vivo," Nat. Photonics **3**(7), 412–417 (2009).
15. S. Y. Emelianov, P. C. Li, and M. O'Donnell, "Photoacoustics for molecular imaging and therapy," Phys. Today **62**(5), 34–39 (2009).

#163769 - $15.00 USD Received 29 Feb 2012; revised 13 Apr 2012; accepted 16 Apr 2012; published 20 Apr 2012

16. C. Zhang, K. Maslov, and L. V. Wang, "Subwavelength-resolution label-free photoacoustic microscopy of optical absorption in vivo," Opt. Lett. **35**(19), 3195–3197 (2010).
17. S. Hu, K. Maslov, and L. V. Wang, "Second-generation optical-resolution photoacoustic microscopy with improved sensitivity and speed," Opt. Lett. **36**(7), 1134–1136 (2011).
18. Z. X. Xie, S. L. Jiao, H. F. Zhang, and C. A. Puliafito, "Laser-scanning optical-resolution photoacoustic microscopy," Opt. Lett. **34**(12), 1771–1773 (2009).
19. G. J. Huang, S. H. Yang, Y. Yuan, and D. Xing, "Combining x-ray and photoacoustics for in vivo tumor imaging with gold nanorods," Appl. Phys. Lett. **99**(12), 123701 (2011).
20. Y. Q. Lao, D. Xing, S. H. Yang, and L. Z. Xiang, "Noninvasive photoacoustic imaging of the developing vasculature during early tumor growth," Phys. Med. Biol. **53**(15), 4203–4212 (2008).
21. K. Maslov, H. F. Zhang, S. Hu, and L. V. Wang, "Optical-resolution photoacoustic microscopy for in vivo imaging of single capillaries," Opt. Lett. **33**(9), 929–931 (2008).
22. Z. L. Tan, Z. L. Tang, Y. B. Wu, Y. F. Liao, W. Dong, and L. N. Guo, "Multimodal subcellular imaging with microcavity photoacoustic transducer," Opt. Express **19**(3), 2426–2431 (2011).
23. H. F. Zhang, K. Maslov, G. Stoica, and L. V. Wang, "Functional photoacoustic microscopy for high-resolution and noninvasive in vivo imaging," Nat. Biotechnol. **24**(7), 848–851 (2006).
24. D. W. Yang, D. Xing, S. H. Yang, and L. Z. Xiang, "Fast full-view photoacoustic imaging by combined scanning with a linear transducer array," Opt. Express **15**(23), 15566–15575 (2007).
25. M. Eghtedari, A. Oraevsky, J. A. Copland, N. A. Kotov, A. Conjusteau, and M. Motamedi, "High sensitivity of in vivo detection of gold nanorods using a laser optoacoustic imaging system," Nano Lett. **7**(7), 1914–1918 (2007).
26. J. A. Copland, M. Eghtedari, V. L. Popov, N. Kotov, N. Mamedova, M. Motamedi, and A. A. Oraevsky, "Bioconjugated gold nanoparticles as a molecular based contrast agent: implications for imaging of deep tumors using optoacoustic tomography," Mol. Imaging Biol. **6**(5), 341–349 (2004).
27. P. C. Li, C. R. Wang, D. B. Shieh, C. W. Wei, C. K. Liao, C. Poe, S. Jhan, A. A. Ding, and Y. N. Wu, "In vivo photoacoustic molecular imaging with simultaneous multiple selective targeting using antibody-conjugated gold nanorods," Opt. Express **16**(23), 18605–18615 (2008).
28. V. P. Zharov, E. I. Galanzha, E. V. Shashkov, N. G. Khlebtsov, and V. V. Tuchin, "In vivo photoacoustic flow cytometry for monitoring of circulating single cancer cells and contrast agents," Opt. Lett. **31**(24), 3623–3625 (2006).
29. N. R. Jana, "Gram-scale synthesis of soluble, near-monodisperse gold nanorods and other anisotropic nanoparticles," Small **1**(8-9), 875–882 (2005).

1. Introduction

Although nanoengineered particles possess great potential for biological and medicinal application, all such materials are subject to a preclinical evaluation process commonly referred to as adsorption, distribution, metabolism, excretion, and toxicity [1,2], which are not yet well defined, stimulating much discussion and research in the area. Therefore, high-resolution visualization of the uptake and the distribution of nanoparticles in organisms is an important issue, especially in the intracellular metabolism research, which will aid to evaluate the affection of nanoparticles to organism [3].

Currently, gold nanorods served as multifunctional-imaging and therapeutic agents have drawn much attention in biomedical research [4,5]. The physical properties of gold nanorods hold a remarkable variance with respect to the surfactant coating, the size, and the shape. Gold nanorods are usually characterized by UV-Vis spectrophotometry, inductively coupled plasma atomic emission spectroscopy (ICP-AES), and transmission electron micros-copy (TEM), but these techniques could not be used for *in vivo* or living cells detection. Confocal reflectance microscopy, Laser confocal fluorescence microscopy and two-photon fluorescence microscopy are the most commonly methods to trace and image the gold nanoparticles for cells imaging [6–8]. Recently, confocal Raman scattering microscopy and photothermal microscopy also have been introduced to detect nano-objects and cellular components [9–12].

Photoacoustic imaging is an emerging biomedical imaging technology that utilizes thermoelastic effect. Energy of the incident pulse laser absorbed by targets partially converts into heat, which instantaneously leads to acoustic waves [13–15]. With an optical objective-focusing light into the biological tissue and an ultrasonic transducer focusing to pick up the photoacoustic signals in the same area, a high resolution image of the tissue can be provided. This approach, referred to as photoacoustic microscopy, has been successfully applied to *in vivo* structural, functional, and molecular imaging [16–18]. Photoacoustic microscopy holds great potential for label-free imaging of melanoma and vasculature because nonfluorescent melanin and hemoglobin are major sources of endogenous absorbers for biological tissue in

#163769 - $15.00 USD Received 29 Feb 2012; revised 13 Apr 2012; accepted 16 Apr 2012; published 20 Apr 2012

the visible and NIR spectral range [19–24]. Though gold nanorods as exogenous contrast agent has been introduced for photoacoustic imaging [25–28], the biological characteristics of free gold nanorods such as uptake and distribution in cells are never reported.

In this paper, we developed a photoacoustic microscope to demonstrate exquisitely high optical-absorption contrast imaging of the nonfluorescent and label-free gold nanorods, which complemented to the fluorescent imaging and arm the *in vivo* detection systems to the nano-biological research. The resolution of the photoacoustic microscope was tested and verified with optical resolution test target. Moreover, nonfluorescent gold nanorods were precisely mapped in single cell. The cell nucleus and the distribution of gold nanorods were clearly identified after H&E staining with dual-wavelength excitation photoacoustic microscopy. Final, the intracellular gold nanorods were monitored, which showed the time-dependent uptake and distribution of the gold nanorods in the cells.

2. Materials and methods

The schematic diagram of the photoacoustic microscopy system is shown in Fig. 1. A tunable pulsed laser source (Vibrant B 532I, Opotek, USA), with wavelengths of 532 and 680-960 nm, a pulse width of 8-10 ns, and a pulse repetition rate of 10 Hz, was used to provide optical illumination. The pulse energy after an optical attenuator was controlled to be ~40 nJ. Laser pulses scanned with a 2D scanning galvanometer (6231H, Cambridge Technology, Inc.) were reshaped by condenser lens and pinhole. Then the laser was focused by an optical objective with 0.85 NA on to sample surface. A focused ultrasonic transducer (SO22, Guangzhou Doppler Electronic Tech. Co., Ltd, China) with a central frequency of 22 MHz, a −6 dB bandwidth of 100%, covered with sound-transparent material of plexiglass was used to receive photoacoustic signals. The transducer was set on the opposing side of the sample to form the confocal mode of laser and ultrasound. The resulting time-resolved photoacoustic wave was detected in transmission mode. Photodiode was used to monitor the output laser for calibration of the energy of each laser pulse. The photoacoustic signals were first amplified 20 dB with an amplifier (ZFL-500, Minicircuits), then digitized by dual-channel data acquisition card (NI 5224, National Instrument, USA) at a sampling rate of 100 MHz, and finally recorded in the personal computer to imaging reconstruction with a MATLAB program (Mathworks, Inc.).

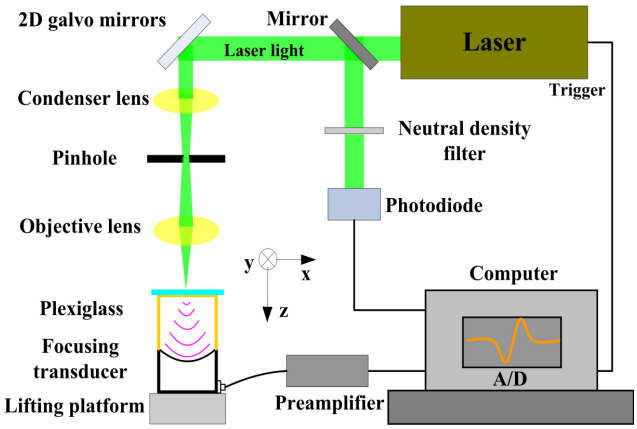

Fig. 1. Experimental schematic of the photoacoustic microscope.

To demonstrate the application of photoacoustic microscopy in imaging of the intracellular nanoparticles with nonfluorescent property, MCF7 cells and gold nanorods were used for the experiments. Gold nanorods were synthesized using a modified nonseeding synthesis protocol [29], which are typically prepared in the presence of cetyltriethylammnonium bromide (CTAB) helping to maintain gold nanorods as stable

#163769 - $15.00 USD Received 29 Feb 2012; revised 13 Apr 2012; accepted 16 Apr 2012; published 20 Apr 2012

dispersions in aqueous solution. The gold nanorods have a longitudinal size of ~60 nm and an aspect ratio of ~2.4, which hold a resonance absorption peak of ~720 nm [19].

Before experiment, the gold nanorods solution was centrifuged twice at 8000 rpm to remove the excess CTAB, and incubated with MCF7 cells in serum-free RPMI 1640 medium for 24 hours under a standard cell growth conditions. The gold nanorods can be internalized into cytoplasm by the endocytosis. Then the cells with gold nanorods were rinsed, fixed and stained with H&E, which can enhance the optical absorption of the cell nucleus. Final, the stained slice was washed with deionized water to remove the extracellular free gold nanorods, hematoxylin and eosin.

For cellular imaging applications, slice glass of sample was put on the top of the focused ultrasonic transducer, and ultrasonic coupling was permeated between slice and transducer for photoacoustic-wave propagation. Laser beam was scanned by the galvanometer in a small imaging field of view, which was overlapped with focal spot of focused ultrasonic transducer. The 2D scanning galvanometer was controlled by a computer, which was triggered by the trigger signals of the pump laser. The whole scan process lasts about 17 minutes. An X-Y-Z scanning stage was used to aline the objective lens, sample and transducer.

3. Results

To measure the transverse spatial resolution of the photoacoustic microscope, gold nanospheres with a diameter of ~60 nm were scanned by the system with 532 nm wavelength laser. The detected photoacoustic amplitude across a gold nanosphere was shown in Fig. 2(a). Then the data were fitted by the theoretical Gaussian function. The lateral resolution of the system, given by the FWHM of the point spread function, is measured to ~500 nm, which is approached to the theoretical value $0.51\lambda/NA \approx 320$ nm. Furthermore, a optical resolution test target with 0.5 μm stripe was used to validate the imaging resolution of the system. Figure 2(b) shows a photoacoustic image of the close-up view on the resolution test target. The right stripe with a space of 0.5 μm was clearly distinguished by the photoacoustic microscope, which is matched well with the optical image of the same scanning area as shown in Fig. 2(c). The experimental result demonstrated that the transverse spatial resolution of the photoacoustic microscope system can reach nano scale for cell imaging.

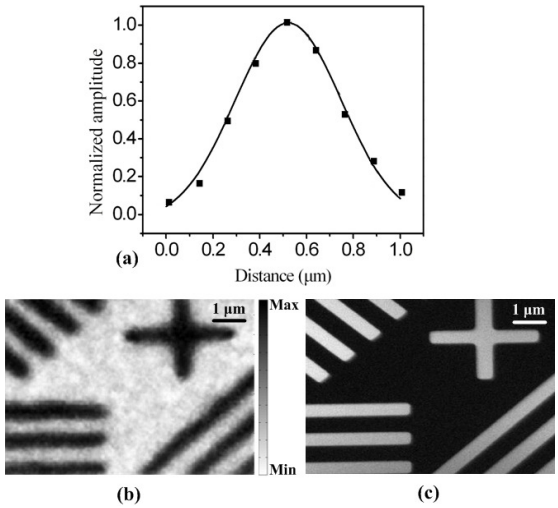

Fig. 2. Transverse spatial resolution of the photoacoustic microscope. (a) Fitting curve of the photoacoustic signal amplitude measured from gold nanosphere. (b) Photoacoustic imaging of a resolution test target. (c) Optical imaging of the resolution test target.

#163769 - $15.00 USD Received 29 Feb 2012; revised 13 Apr 2012; accepted 16 Apr 2012; published 20 Apr 2012

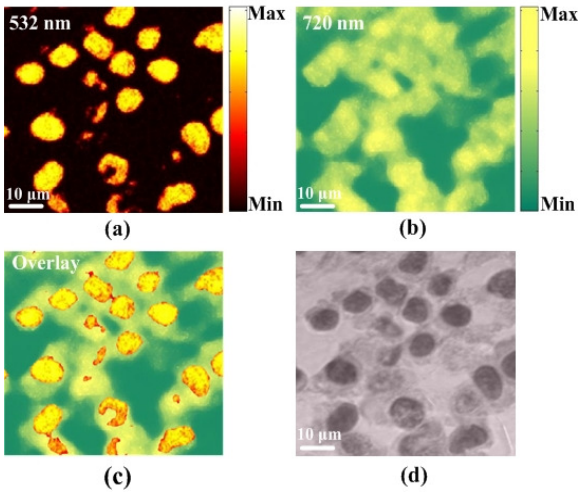

Fig. 3. Photoacoustic microscopic imaging of cells and the intracellular gold nanorods. (a) Photoacoustic image of cell nucleus with excitation wavelength of 532 nm laser. (b) Photoacoustic image of gold nanorods in the cytoplasm with excitation wavelength of 720 nm laser. (c) Overlay image of (a) and (b). (d) Photograph of the H&E stained cells sample.

The photoacoustic microscopic imaging of the H&E-stained cells sample containing the gold nanorods was shown in Fig. 3. Figure 3(a) and (b) provide the photoacoustic images of MCF7 cells highlighted on cell nucleus and gold nanorods by different excitation laser wavelengths of 532 and 720 nm, respectively. With H&E staining, the cell nucleus of MCF7 cells was stained in purple, thus high-contrast photoacoustic imaging of cell nucleus can be obtained with green laser excitation. Similarly, photoacoustic imaging of intracellular gold nanorods can be acquired by the excitation with the peak absorption wavelength of the particles. Figure 3(a) presents sharp boundary and high contrast for the cell nucleus, while Fig. 3(b) shows a relatively vague profile of the cells, which is likely determined by concentration and distribution of gold nanorods in the cells. A more informative visualization including the cell morphology and distribution of the intracellular gold nanorods was shown as the overlap image of Fig. 3(c), which agrees well with the sample photograph shown in Fig. 3(d). The results demonstrated that the nonfluorescent gold nanorods inside the cells can be detected and visualized clearly with dual-wavelength photoacoustic microscopy.

To further demonstrate photoacoustic microscopy monitoring of the uptake and distribution of gold nanorods in the cells, the samples of MCF7 cells incubated with gold nanorods for 2 h, 6 h and 24 h were shown to photoacoustic examination, respectively. Fluorescent imaging of the samples were also provided as a control.

Based on the endocytosis, the internalization of gold nanorods in MCF7 cells shows a time-dependent process seen in Fig. 4(a-c). The gray scaling in all the photoacoustic images refers to the same range of absolute signal strength. Cell uptake of gold nanorods can be found after 2 h incubation, and gold nanorods began to gather in the cytoplasm (Fig. 4(a)). After 24 h incubation, the intracellular gold nanorods were revealed with high photoacoustic intensity. The distribution of gold nanorods in cytoplasm can be easily distinguished for the cell contour with a low-light area in the center (marked with arrows in Fig. 4(c)), which could probably be the cell nucleus. Quantitative analysis of photoacoustic signal intensity of the intracellular gold nanorods with different incubation time was shown in Fig. 4(e), which further validated the uptake concentration of gold nanorods are proportional to the incubation time. Figure 4(d) shows the fluorescent imaging of the incubated cells sample with 24 h, but there is no fluorescent signals in the cells can be found. The experimental results demonstrated a great example for photoacoustic microscopy of nonfluorescent nanoparticles.

#163769 - $15.00 USD Received 29 Feb 2012; revised 13 Apr 2012; accepted 16 Apr 2012; published 20 Apr 2012

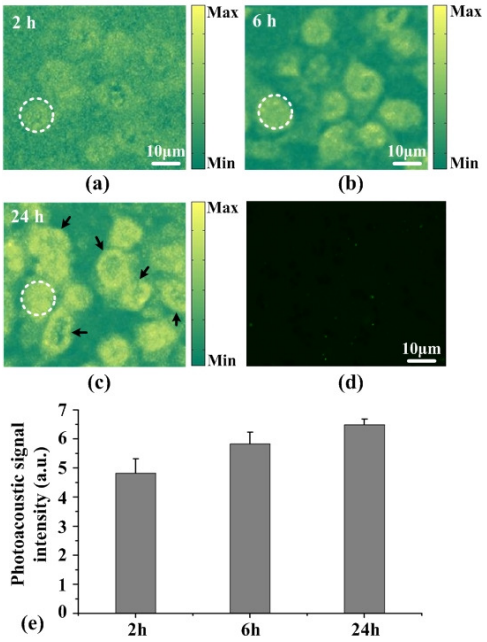

Fig. 4. Photoacoustic monitoring of the uptake of intracellular gold nanorods with incubation of MCF7 cells for 2h (a), 6h (b) and 24h (c). (d) Fluorescent imaging of intracellular gold nanorods in MCF7 cells. (e) Photoacoustic signal intensity of the white cycle in (a), (b) and (c).

4. Discussions and conclusions

Nonfluorescent gold nanorods in cells were first visualized and continuous monitored by the home-made photoacoustic microscope. Though the photothermal microscopy holds higher sensitivity and better spatial resolution, the photoacoustic microscopy may provide deeper imaging by detection of ultrasonic in tissues. In this paper, though the samples were fixed in the experiments, the imaging of cells can reflect the realized state as like biopsy. For *in vivo* imaging, the scanning optical path can be further optimized to improve the spatial resolution, which would help to avoid biological heating damage. In addition, an advanced transducer with higher sensitivity and higher frequency as well as low-resistance electronic devices would enhance the detection sensitivity of the system to reduce the excitation laser power. In summary, a home-made photoacoustic microscope was developed and provided high optical-absorption contrast imaging. Cell nucleus and intracellular gold nanorods were observed simultaneously in single cell with dual-wavelength photoacoustic microscopy. The uptake and the distribution of gold nanorods in the cells were monitored with different incubation time. Photoacoustic microscopy can directly detect the nonfluorescent gold nanorods, which are no need to conjugate with fluorescent molecular. Our results provide a superior method to monitor the label-free nanoparticles, which will help the intracellular photodynamic therapy and drug delivery research.

Acknowledgments

This research is supported by the National Basic Research Program of China (2011CB910402; 2010CB732602), the Program for Changjiang Scholars and Innovative Research Team in University (IRT0829), the National Natural Science Foundation of China (81127004, 11104087, 30870676), the Foundation for Distinguished Young Talents in Higher Education of Guangdong, China (LYM10061), and Specialized Research Fund for the Doctoral Program of Higher Education (20114407120001).

#163769 - $15.00 USD Received 29 Feb 2012; revised 13 Apr 2012; accepted 16 Apr 2012; published 20 Apr 2012